Pectin and Polyacrylamide Composite Hydrogels: Effect of Pectin on Structural and Dynamic Mechanical Properties

Linshu Liu, Peter H. Cooke, David R. Coffin, Marshall L. Fishman, Kevin B. Hicks

U.S. Department of Agriculture, ARS, Eastern Regional Research Center, 600 East Mermaid Lane, Wyndmoor, Pennsylvania 19038

Received 16 January 2003; accepted 20 November 2003

ABSTRACT: Composite hydrogels of pectin and polyacrylamide were synthesized and evaluated by scanning electron microscopy, atomic force microscopy, light microscopy, and dynamic mechanical analysis. The crosslinking polymerization of acrylamide in pectin solution resulted in a composite having a macroporous pectin domain with an interstitial polyacrylamide domain. This composite had improved mechanical properties compared to those of either polymer alone, and it absorbed and retained more water than crosslinked polyacrylamide alone. Furthermore, crosslinking polymerization of acrylamide in an existing pectinate scaffold resulted in a double-network architecture, where filamentous polyacrylamide networks penetrated through pores of the pectin scaffold. It was found that pectins dictated the features of microstructure in the composites through regulating the coordination of phase separation of the two components and water partition between the two phases. Results from this study highlight potential new uses of pectins in protecting the physical structure of environmentally sensitive polymers from mechanical damage related to freezing, lyophilization, and other conditions experienced during their use in biomedical and industrial products. © 2004 Wiley Periodicals, Inc. J Appl Polym Sci 92: 1893–1901, 2004

Key words: pectin; polyacrylamide; composites; hydrogels; microstructure

INTRODUCTION

Pectin-derived hydrogels swell in solutions at high pH and shrink at low pH, offering a great opportunity for use in controlled delivery of bioactive substances,[1] in the food industry,[2] and soil and water preservation.[3] Combining pectin with a second polymer into composites can create unique properties and extend practical applications for the pectin composite systems compared to each polymer alone.[4,5] The formation of composite hydrogels involves a series of complicated and coordinated physicochemical processes, such as changes in hydrodynamic properties of each polymer, phase separation, and water partition. Physical and chemical interactions between individual components determine the structure and properties of the composite hydrogel. Water partition within the hydrogel strongly influences the response of the hydrogel to external changes in temperature or electric field, to stimuli from solvent composition, to biological reactions, and to light irradiation.[6–12] Hydrogels have been applied to the study of separation processes.[13,14] Other areas of application in which hydrogels are scientifically and economically important are agriculture, pharmaceuticals, biotechnology, tissue engineering, and robotics.[7–9,11,15,16] Recently, hydrogels with specific architectures have been developed to respond to needs for high-efficiency media and for materials with new functionality and lower cost.[17–19] Attention and resources have mostly been focused on the efforts to regulate the microstructures of individual phases and on the entire architecture of composites. Studies of water partition occurring in composite hydrogels have increased the understanding of the relationship between the structure and physical properties of the composite. For practical reasons, polyacrylamide hydrogels are often chosen as a model study system.

In this study, the use of pectin to regulate water partition in composite hydrogels was studied. Two methodologies for preparing composite hydrogels from pectin polymers and acrylamide monomers were studied. The microstructure of composite hydrogels was evaluated by means of microscopy, the rheology by mechanical properties, and the capacity to absorb and retain water by water content. In this study, we focused particularly on the effect of the physical status of pectin on the microstructures of the polyacrylamide phase and on the entire architecture of the composites.

EXPERIMENTAL

Materials

Sodium pectinate [Grindsted®, MW 90,000; degree of esterification (DE) 60%] was obtained from Danisco

Mention of brand or firm name does not constitute an endorsement by the U.S. Department of Agriculture above others of a similar nature not mentioned.

Correspondence to: L. Liu (lsliu@arserrc.gov).

Journal of Applied Polymer Science, Vol. 92, 1893–1901 (2004)
Published by Wiley Periodicals, Inc.

(Danisco Cultor USA, New Century, KS). Acrylamide, bismethylene-acrylamide, and *N,N,N,N'*-tetra-methylethylenediamine (TEMED) were purchased from Bio-Rad (Hercules, CA). Ammonium persulfate (APS), methylene blue, and calcium chloride were from Aldrich (Milwaukee, WI).

Preparation of pectin and polyacrylamide gels

Polyacrylamide gels were prepared from a 2 mol/L solution of acrylamide and 32 m*M* bismethylene-acrylamide. To polymerize acrylamide, the solution was degassed followed by the addition of 2.2 m*M* APS and 3.3 mmol/L TEMED. The solution was poured into a petri dish to form a layer 4 mm thick. Gels thus prepared were lyophilized and labeled as P_1.

Pectin gels were cast in 96-well microtiter plates (Fisher Scientific, Pittsburgh, PA). Each well contained 120 μL of pectin solution, 20 mg/mL in deionized water (D.I. water). The solution was degassed, incubated at 4°C for 2 h, frozen at −20°C for 4 h, and lyophilized to create a spongelike, porous structure. The dry matrices were immersed in 0.1 mol/L $CaCl_2$ to insolubilize the pectin and to fix the three-dimensional features of the gel. Gels were washed with a large volume of D.I. water with several changes, lyophilized again, and labeled as P_2.

Pectin/polyacrylamide gels were prepared by polymerizing acrylamide and bismethylene-acrylamide in pectin solution together in one step. One volume of pectin solution (4%, w/v) was mixed with an equal volume of solution containing acrylamide (4*M*) and bismethylene-acrylamide (64 mmol/L). The mixed solution was degassed followed by addition with 4.4 mmol/L APS and 6.6 mmol/L TEMED. The solution was then quickly mixed and poured into a cylindrical polypropylene tube (diameter: 9 mm; Fisher Scientific), covered with parafilm at both ends, allowed to stand at ambient temperature for 2 h, then lyophilized. The gels were removed, immersed in 0.1 mol/L $CaCl_2$ at ambient temperature for 1 h, washed with a large volume of D.I. water, and lyophilized again. Gels thus prepared are labeled as P_1P_2I.

Alternatively, pectin/polyacrylamide gels were prepared by a two-step method from the lyophilized preformed pectin gels, P_2, and the solution of 2 mol/L acrylamide and 32 mmol/L bismethylene-acrylamide. The gels and the solution were degassed separately. APS and TEMED were added to the solution, mixed vigorously, and then injected into pectin gels using a pipet, 120 μL for each. After polymerization, the gels were lyophilized and labeled as P_1P_2II.

In another experiment, wet P_2 gels were prepared by incubation of dry P_2 matrices in D.I. water for 2 h at ambient temperature, then removed from the water, placed on tissue papers, and compressed gently to remove residual water in the pore spaces of the gels. The gels thus treated were injected with 80 μL of acrylamide solution with the same compositions as used for P_1P_2II preparation. After polymerization the gels were lyophilized and labeled as P_1P_2III.

In still another experiment, an acrylamide solution of the same compositions as used for P_1P_2II preparation was poured onto the surfaces of a dry P_2 matrix, polymerized at ambient temperature followed by lyophilization, and labeled as P_1P_2IV.

Scanning electron microscopy (SEM)

For SEM examination, samples were dehydrated by immersion in absolute ethanol and frozen in liquid nitrogen. After 5 min of freezing, samples were fractured manually with the edge of a cooled scalpel blade. Sample fragments were thawed in absolute ethanol and critical-point dried from liquid carbon dioxide. Dry fragments were mounted on aluminum specimen stubs with colloidal silver adhesive (Electron Microscopy Sciences, Ft. Washington, PA) and coated with a thin layer of gold by dc sputtering. Images of topographical features in fracture faces were made using a model JSM 840A scanning electron microscope (JEOL USA, Peabody, MA) coupled to an Imix-1 digital image workstation (Princeton Gamma-Tech, Princeton, NJ).

Optical microscopy

For correlative imaging with SEM, optical images of sample fragments were made (before sputter coating with gold) by reflected light from a model 190 fiber optic illuminator (Dolan-Jenner, Woburn, MA) and a model MZ FLIII stereomicroscope (Leica Microscopy Systems, Heerbrugg, Switzerland) equipped with a color CCD camera.

Atomic force microscopy (AFM)

Sample fragments, similar to those freeze-fractured and critical-point dried for SEM, were cemented to metal disks and imaged in a model Nanoscope IIIa scanning probe microscope with TESP cantilevers (Veeco/Digital Instruments, Santa Barbara, CA) operated in the intermittent contact mode on an atomic force microscope.

Mechanical test

Compressive mechanical testing of the samples was performed on a Rheometric Scientific RSA II Solids Analyzer (Rheometric Scientific, Piscataway, NJ). The test fixture consisted of two 25-mm parallel plates. Most of the samples tested had been prepared in the 96-well microtiter plate described above, and had nominal dimensions of 5.5 × 3.5 mm (d × h). For P_1P_2I

the test specimen was cut from the freeze-dried cylindrical sample. The samples were placed on the lower plate and the upper plate was lowered onto the sample to give a slight compressive force. The upper plate was then locked in place. The samples were tested using a compressive strain of 0.25 to 1.0% depending on the sample. The samples were tested using a temperature ramp from −100 to +200°C at a heating rate of 10°C/min. Storage modulus, loss modulus, and loss tangent were determined for the samples over this temperature range. The data were analyzed using Rheometric Scientific Orchestrator software, version 6.5.7.

Water content and retention

Swelling studies were carried out at ambient temperature using specimens of the same size as those applied for mechanical testing. Specimens of all samples were freeze-dried for 48 h, weighed (W_d), and transferred into large volume of D.I. water. At regular intervals, specimens were removed from the water, wiped with tissue paper to remove the excess water adhering to the surface, weighed (W_w), and reimmersed in the water. This process was repeated until the specimens attained a constant weight. The water content was calculated as $(W_w - W_d)/W_w$.[6]

To test water retention, specimens, 500 mg for each sample, were evenly seeded on petri dishes (50 × 11 mm; Fisher Scientific, Pittsburgh, PA) and 10.0 g of D.I. water was added. The dishes were placed in an incubator and incubated at 25°C under a humidity of 18–21%. After 24 h, the weight loss of the contents in each petri dish was recorded. Ignoring the influence of the elevation in Philadelphia, PA on gravity, the rate of water evaporation (r) was calculated and expressed as r = mm/h. Plain petri dishes containing water were used as control.

Experiments for water content and retention were carried out four times for each sample. Data are expressed as the mean ± SD. Significance was determined with the use of a Student's t-test.

RESULTS

In the present study, acrylamide monomers were polymerized either in a solution of dissolved pectin or in an existing structure of pectin that was insolubilized by calcium. The morphology of the resulting composites was investigated by microscopy and dynamic mechanical testing. These methods allowed us to characterize such composite features as the domain size and shape of each component, the microstructure and continuity of each phase, and composite global structural and mechanical properties.

Electron microscope characterization of composites

Micrographs of polyacrylamide (P_1) and pectin/polyacrylamide composite (P_1P_2I) are shown in Figure 1. SEM [Fig. 1(A)] and AFM [Fig. 1(B)] revealed that the frozen-fractured faces of freeze-dried polyacrylamide alone (P_1) were multifaceted on a macroscopic scale [Fig. 1(A), (B)]. Facet widths ranged from less than 0.1 mm to over 2 mm. Figure 1(A) revealed that individual facets in the fracture face were very smooth except for small circular depressions between 50 and 100 nm wide and deep. When circular depressions were absent, irregular clusters with dimensions around 200 nm were observed (data not shown). Fracture faces of P_1P_2I composites have a macroscopic structure that is very similar to that of polyacrylamide alone [cf. Fig. 1(A), (C)]; the frozen-fractured faces are multifaceted on a macroscopic scale, but the facets are larger and separated only by discrete circular holes or discoidal clefts ranging from 10 to 100 μm wide. Areas around the borders of the holes and clefts were very smooth topographically, and regions between these open areas were identical to the clusters and circular depressions in the microstructure of polyacrylamide alone. P_1P_2I composites were made with the addition of methylene blue to identify the pectin component through correlative optical color imaging [Fig. 1(D)] and SEM [Fig. 1(E)]. Comparison of these two figures indicates that the areas around the holes and clefts correlate with pectin, which stains blue, whereas intervening solid regions were colored white as expected for polyacrylamide that is not stained by methylene blue. The white color arises from the numerous small depressions or other light-scattering surfaces. These results indicate that the P_1P_2I composite is a macroporous material with pectin lining hollow pores and polyacrylamide filling the large interstices between pores.

The organization and microstructures of sample P_2 and the combined components P_1P_2II are illustrated in Figure 2. Figure 2(A) is an SEM micrograph showing the frozen-fractured faces of freeze-dried pectin gel alone, P_2. Figure 2(A) reveals a regular porous organization, resembling the natural tissue cell structure in plant organs, notably potato tubers and citrus fruits.[20,21] The pectin was arranged into a continuous and regular system of walls or sheetlike partitions containing open pores around 100 μm in diameter [Fig. 2(A)]. The walls lining these cellular spaces were less than 1 μm thick and formed numerous triangular junctions resembling the middle lamella of plant cell walls. Some cellular pores or spaces contained circular apertures or openings into adjacent spaces. The surface of cavity walls was further probed by AFM [Fig. 2(B)]. AFM imaging revealed that the surface of the walls or sheetlike partitions were composed of a flat but complex arrangement of short fibrils and/or gran-

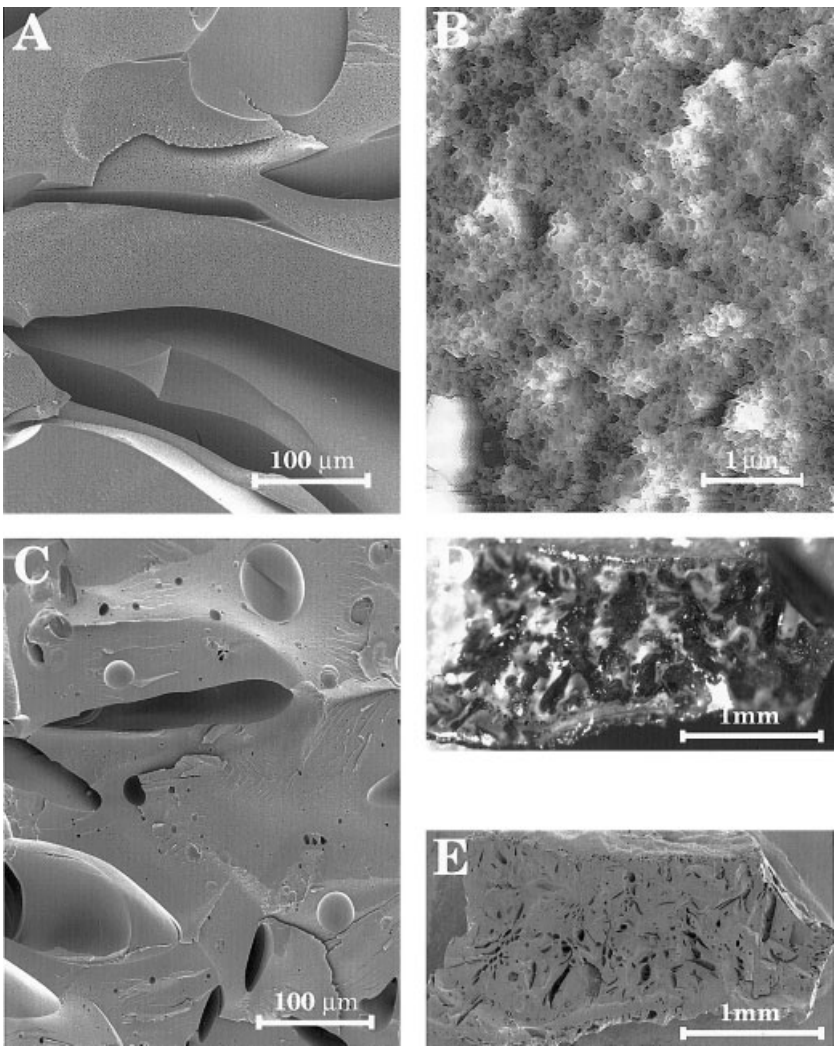

Figure 1 (A) SEM photograph of frozen-fractured polyacrylamide gels (P_1), bar = 100 μm. (B) AFM on P_1 gels, bar = 1 μm. (C) SEM image of frozen-fractured pectin and polyacrylamide composite gels, P_1P_2I, bar = 100 μm. (D) Image of light microscope of P_1P_2I gels after staining with methylene blue, bar = 1 mm. (E) SEM image of the correlative area shown in (D), bar = 1 mm.

ules ranging from 20 to 30 nm wide [Fig. 2(B)]. The AFM image may suggest complex aggregates of pectin molecules that are randomly arranged in the plane of the walls. When polyacrylamide was injected into the regular porous, cellular structure of pectin, loose, microporous networks of fine strands were located within and between many of the cellular spaces. These strands are composed of strings of small granules, around nanometer scale in diameter [Fig. 2(C)].

The organization and microstructure of P_1P_2III and P_1P_2IV are illustrated in Figure 3. Polyacrylamide, formed in a wet, porous pectin gel, has a nonwoven network structure [Fig. 3(A), (C)]. In contrast to those formed in dry pectin structure, the acrylamide networks in the P_1P_2III composite consist of beltlike, flat strands with widths on a micrometer scale. The strands have very smooth surfaces, similar to the facets found in the fracture face of gels containing only polyacrylamide. The pores created in the polyacrylamide structure in P_1P_2III composite are irregular in shape, ranging from 1 to 2 μm in width. Polyacrylamide formed on the surface of dry pectinate matrix displays a network structure similar to that observed in P_1P_2I composites [cf. Fig. 2(C) with Fig. 3(B)].

Compression test

Typical compressive storage modulus (E'), loss modulus (E''), and loss tangent (tan δ) curves are compared for each sample in Figure 4. The freeze-dried polyacrylamide matrix and the two-step pectin/polyacrylamide composite (P_1P_2II) had fairly similar curves for the storage modulus, and exhibited peaks at 113 and 97°C, respectively. The one step pectin/polyacrylamide (P_1P_2I) was somewhat similar, but had two noticeable differences. The initial modulus behavior

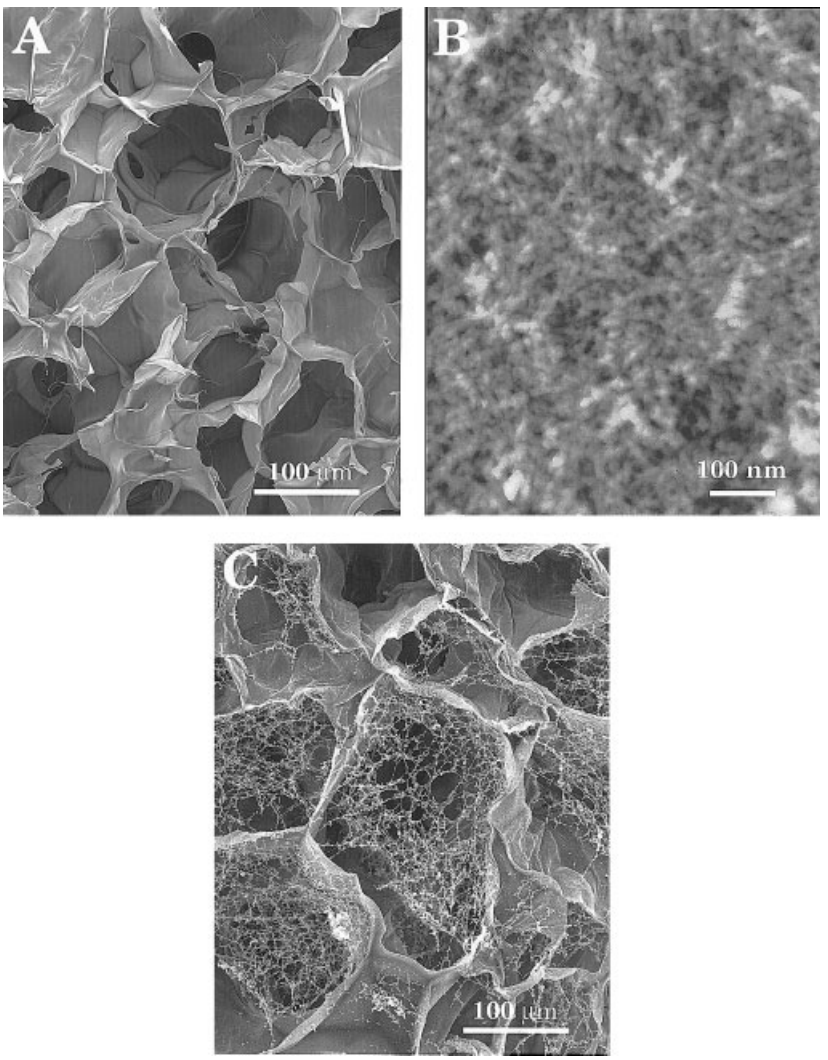

Figure 2 (A) SEM image of frozen-fractured crosslinked pectin gels (P_2), bar = 100 μm. (B) AFM image of frozen-fractured P_2 gels, bar = 100 nm. (C) SEM image of pectin and polyacrylamide composite gels (P_1P_2II), bar = 100 μm.

from −95 to +75°C showed the same flat curve as that of the other two samples, although the value obtained was about 50% higher. A peak occurred at about 93°C, and the modulus dropped significantly below the other curves by 125°C. The curve for the pectin matrix was relatively flat, with a broad minimum at about 13°C. This curve was well below that of the other three over most of the temperature range; however, at about 135°C the curve for P_1P_2I dropped below it. By 200°C the other two curves had dropped to the approximate value of the pectin matrix.

The loss modulus behavior was somewhat different [Fig. 4(B)]. The P_1P_2I and P_1P_2II matrices gave roughly similar curves with large peaks at 105 and 121°C, respectively. The matrix of polyacrylamide alone gave a smaller peak at about 133°C. From −100 to about 55°C all three samples had comparable modulus values. As in the case of the storage modulus, the loss modulus value for P_1P_2I dropped significantly after the peak. The pectin curve again had much lower modulus values, and showed two broad maxima at −51 and +81°C, and one broad minimum at 13°C. By 200°C the value for P_1P_2I was down to that of the pectin.

The loss tangent behavior [Fig. 4(C)] was overall rather similar to that seen for the loss modulus. The peaks for the polyacrylamide, P_1P_2I, and P_1P_2II matrices were at about 141, 133, and 129°C, respectively. They also had the same relative sizes as they had in the loss modulus curves. The pectin curve had a broad maximum at about 21°C.

Overall, the dynamic mechanical behavior of the polyacrylamide and the two pectin/polyacrylamide matrices was fairly similar. As a group they were very distinct from the pectin-only matrix. The glass-transition temperatures of the polyacrylamide-containing matrices, as measured by the peak in the loss tangent curves, were in the range of 129–141°C. These are

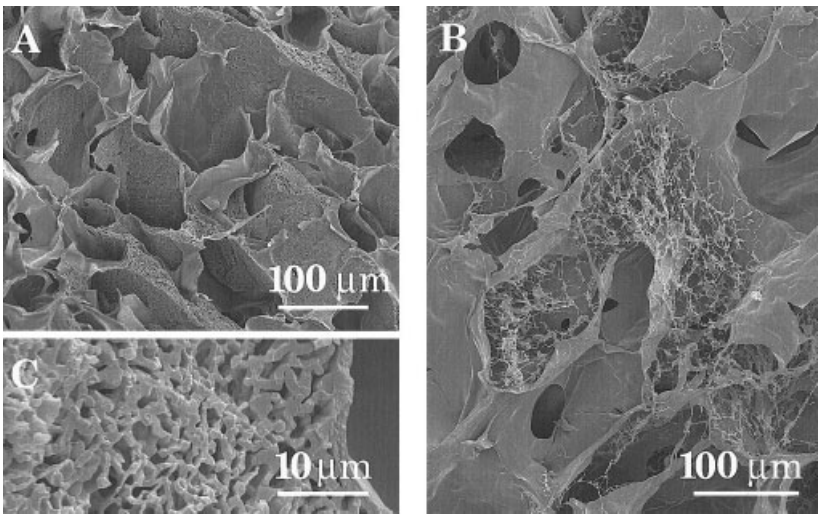

Figure 3 (A) SEM image of frozen-fractured pectin and polyacrylamide composite gels (P_1P_2III), bar = 100 μm. (B) SEM image of frozen-fractured pectin and polyacrylamide composite gels, P_1P_2IV, bar = 100 μm. (C) SEM image of frozen-fractured P_1P_2III gels in high magnification, bar = 10 μm.

comparable to the value of 165°C reported in the *Polymer Handbook*.[22] The presence of the pectin in the two samples probably accounts for their lower glass-transition values. The P_1P_2I sample appears to be made so as to have a higher density than that of the other samples. This may account for the higher storage modulus values seen for it below the glass-transition temperature.

Water content and retention

The hydration behavior of the four types of hydrogels—P_1, P_2, P_1P_2I, and P_1P_2II—were determined in terms of the ability to absorb and retain water. The results summarized in Table I revealed that P_2 and P_1P_2II absorbed about the same amount of water. Both of the gels have remarkable water-absorbing capacity, ranging from 34 to 36 times the weight of dry matrices. In addition, both P_2 and P_1P_2II are able to maintain the absorbed water for a period longer than that observed with P_1 and P_1P_2I gels, given that the absorbed water evaporated from P_2 and P_1P_2II at the lowest rate. Although there is only a slight difference in water retention found between P_1 and P_1P_2I gels, the P_1P_2I composite gel absorbed more water than did the P_1 gel.

DISCUSSION

In this study we investigated the effect of pectin on the architecture of pectin and polyacrylamide composite hydrogels, particularly on the microstructure of polyacrylamide phases in the composites. Pectin—specifically, pectinic acid—is a polyacid. The intermolecular interaction between a polyacid and polyacrylamide is dependent on (1) the ionization of polyacid and (2) the structural compatibility between the polymers. At low ionization, polyacids function as hydrogen donors, and thus can intermolecularly hydrogen-bond to polyacrylamide, which is a proton acceptor, to form an intermolecular complex. At some point as ionization increases, the two polymers will act independently. A model system to demonstrate this kind of behavior is the polymerization of acrylic acid or methacrylic acid in the presence of polyacrylamide.[23–25] The polyacrylic acid and polyacrylamide are compatible with each other, both are highly water soluble, and their molecular chains are highly flexible. Thus, the intermolecular interaction between the two polymers is efficient as the polyacids are deionized, and the two polymers mix at segment level or at molecular level, resulting in an interpenetrating network (IPN) structure. Pectin is a natural polyacid, but it has a completely different chemical structure than that of polyacrylic acid. The backbone of pectin consists predominantly of poly(galacturonic acid) blocks interrupted by inserted rhamnose segments with attached neutral sugar branches. The galacturonic acid is methyl esterified to various degrees, depending on the sources of pectin. The number and the distribution of carboxylic groups along the backbone chains of pectin, as well as the side branches, specifically control the electrostatic properties and viscometric behavior of the polymer.[26]

In the current experiments, the pectin has a DE of 30% and its residual carboxylate groups are in the sodium form. In aqueous solution, pectin polymers may exist as a complex mixture of associated network structures, branched structures, and linear structures in the form of rods, segmented rods, and kinked rods.[27–30] These chemical and physical structures of

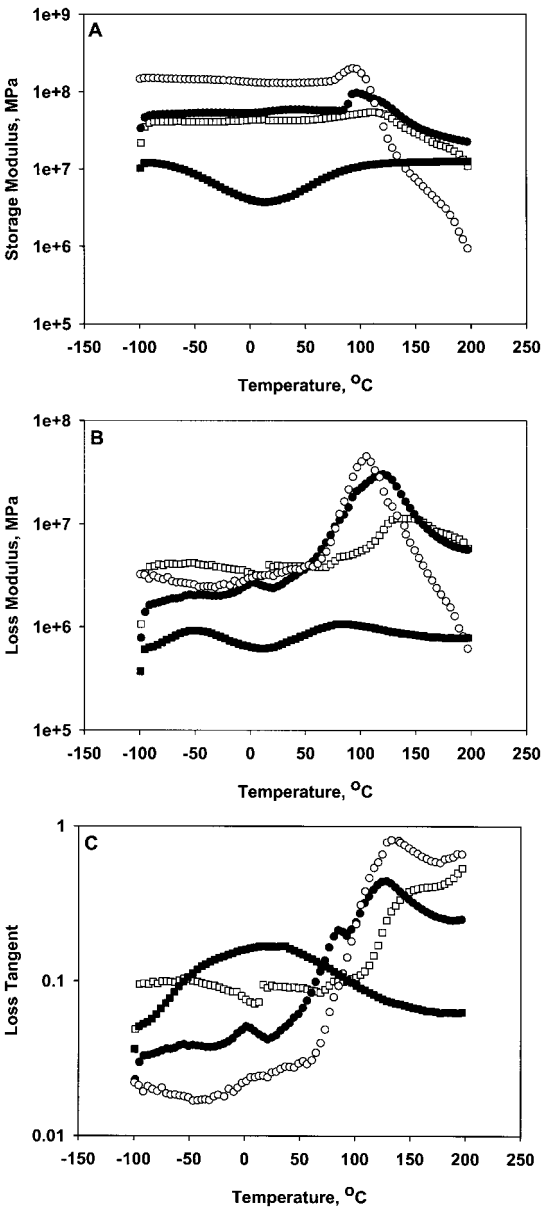

Figure 4 Typical plots of (A) storage modulus, (B) loss modulus, and (C) loss tangent as a function of temperature. P_1 gels, (□); P_2 gels, (■); P_1P_2I gels, (○); P_1P_2II gels, (●).

pectin may inhibit the hydrogen-bonding between pectin and polyacrylamide. Furthermore, the differences in the structure and solubility between the two polymers contribute to their incompatibility and the water partition in the polymer–water heterogeneous system. As expected, the polymerization of acrylamide in the presence of a viscous pectin solution resulted in a heterogeneous composite (P_1P_2I gel) instead of a complex with IPN structure. As the polymerization progressed, the newly formed hydrogel entrapped pectin inside the network and forced it to further aggregate. Networks of pectin macromolecules tend to entrap a large volume of water to balance the osmotic pressure and to buffer the electrostatic repulsion rising from their pendent anionic groups.[31–33] Thus, the water distribution between the pectin phase and the acrylamide phase was found to be uneven. This was demonstrated by SEM examination. As illustrated in Figure 1(B) and (C), there is a larger pore volume in the pectin phase than in the acrylamide phase. Furthermore, pores in the pectin phases are larger than those found in the acrylamide phases. Possibly, these pore spaces were created by entrapped water that was removed by lyophilization.

Accompanying the water partition to the pectin phase, the aggregates of pectin macromolecules should tend to disentangle from the network to form a separated pectin layer and a polyacrylamide layer. On the other hand, the polyacrylamide networks tend to shrink and repack the polymer chains in a denser and clustered pattern. Ultimately, the tightly packed acrylamide zones prevent the escape of pectin aggregates. As shown in Figure 1(C)–(E), these two phases are tightly packed together. At the adjacent areas of phases, the two polymers closely approach and adhere to each other. Apparently, the water partition to the pectin phase increases the density of the polyacrylamide phase. This may contribute to the increase in storage modulus and the decrease in loss tangent of P_1P_2I composites compared with that measured from dry P_1 matrices (Fig. 4). In response to the surrounding heavy polyacrylamide phases, the pectin phase also developed a relatively dense structure after lyophilization, differing from what was observed in native plant cell walls and from what developed from pectin solutions [Fig. 2(A)].

In the absence of acrylamide, the lyophilization of a pectin solution created a three-dimensional porous scaffold. The structure, under SEM, exhibits a repeating network of solvent cavities at the size of about 100 μm and polymeric strands at the size of 1 μm [Fig. 2(A)]. Because the thickness estimated for an individual pectin strand is between 0.5 and 0.8 nm by AFM method[34] and around 1 nm by X-ray scattering method,[35,36] data from this study suggest that the wall of

TABLE I
Characteristics of Pectin-Based Gels for Water Absorbing and Desorbing[a]

Sample ID	Water content[b] (%)	Rate of water evaporation (mm/h)
Control	NA[c]	0.203 ± 0.017
P_1	79 ± 3	0.173 ± 0.008**
P_2	98 ± 3	0.144 ± 0.012
P_1P_2I	88 ± 2	0.157 ± 0.007**
P_1P_2II	97 ± 4	0.137 ± 0.011

[a] Data are expressed as mean ± SD ($n = 4$). **$p < 0.01$; for others, $p < 0.05$.
[b] Not submitted to statistic analysis.
[c] NA, not applicable.

cavities may represent aggregates of a huge number of polymer molecules. This conclusion arises from AFM images, which revealed an arrangement of short fibrils and/or granules in the construction of the cellular walls [Fig. 2(B)]. Furthermore, SEM images [Fig. 2(A)] reveal that numerous triangular junctions were formed in the adjacent areas of cavities, mimicking the structure of middle lamella of plant cell walls. Such an organization would potentially enhance the physical strength of the gel structure. Indeed, the pectin scaffold is able to maintain its three-dimensional structure even after it is filled with an acrylamide solution, which is followed by polymerization of the acrylamide and lyophilization of the composite that results [Fig. 2(C)].

The compressive mechanical properties as a function of temperature were determined by dynamic mechanical analysis (DMA) for pectin, polyacrylamide, and their composites (Fig. 4). The initial decrease in the E' value of the pectin aero gel (P_2) with increasing temperature [Fig. 4(A)] may reflect segmental motion of pectin molecules attributed to an incipient glass transition. This may indicate that the $CaCl_2$ insolubilization of pectin with minimal crosslinking occurred. Thermal energy in combination with decreased polymer–polymer interactions attributed to air spaces could allow destructuring the pectins' spongelike structure. The recovery of E' to its initial value at higher temperatures may result from losses in air spaces to an extent that permits increased polymer–polymer interactions. Previously, we found that the tensile storage modulus E' for neat high methoxyl pectin films was practically constant over the temperature ranging from -100 to 200°C, which was explained by strong cooperative polymer–polymer interactions attributed to hydrogen bonding.[37] The data in Figure 4 reveal that lyophilized polyacrylamide unlike lyophilized pectin undergoes a glass transition in the 130 to 140°C range. This behavior would indicate that in the absence of air spaces that cooperative intermolecular hydrogen bonding is stronger for pectin than for polyacrylamide. Nevertheless at lower temperatures where air spaces are present in lyophilized pectin, cooperative intermolecular hydrogen bonding is stronger for polyacrylamide than for pectin.

The crosslinking of acrylamide monomers in the dry pectin scaffolds resulted in another porous network penetrating through the pectin networks. Thus, the P_1P_2II gels have a double-network structure, which contributed to the increase in E' value and the decrease in E'' value of P_1P_2II composite gels obtained from small deformation testing (DMA) (Fig. 4). This complex structure was observed using SEM even after lyophilization. It is rather surprising that P_1P_2I and P_1P_2II have similar DMA in that P_1P_2II is more porous than P_1P_2I. It would appear that crosslinked networks of polyacrylamide within pectin pores are as efficient at preventing the onset of molecular motion with increasing temperature as is increasing the packing density, which occurs with P_1P_2I.

Water partition between the solid pectin phase and the liquid polyacrylamide phase is considered to play a key role in the construction of the composite. The dry pectin scaffolds demonstrated the highest capacity to absorb and retain water (Table I) among the four hydrogels. Therefore, the water entrapped in polyacrylamide gels, which is located in the pore spaces of pectin scaffolds, is supposedly absorbed by the walls of pores before the process of lyophilization. We speculate that the porous pectin structure not only provides spaces for the deposition of polyacrylamide gels, but also functions as a blotting paper to remove the water held by the polyacrylamide gel. To verify this hypothesis, acrylamide was allowed to polymerize and crosslink inside a pectin scaffold, P_1P_2III. In this experiment the walls of the pectin scaffold were saturated with water but little or no water was allowed to remain in the pore spaces. Therefore, water absorbed in the pectin walls inhibited the transfer of water from the acrylamide phase to the pectin phase. The resulting polyacrylamide shows a tightly packed network-like structure [Fig. 3(A), (C)], which combines the characteristics of polyacrylamide phases observed with P_1P_2I and P_1P_2II composite hydrogels. In another experiment, a solution of acrylamide monomers was laid on the top of a dry porous pectin scaffold (P_1P_2IV) and allowed to polymerize and lyophilize. A polyacrylamide network of filamentous polymer strands was obtained [Fig. 3(B)], resembling the structure found in P_1P_2II composite hydrogels [Fig. 2(C)]. Results from the above experiments confirm that to maintain the physical structure of crosslinked polyacrylamide, it is critical to remove entrapped water in the polyacrylamide hydrogel by transferring it to dry pectin. Furthermore, this should be done before subjecting the composite to lyophilization.

CONCLUSIONS

The microstructure of pectin and polyacrylamide composite hydrogels could be determined by the physical status of pectin, which regulated the coordination of water partition and phase separation in the composites. The water partition from a liquid polyacrylamide phase to another liquid pectin phase resulted in a composite with tightly packed structure. The water partition from a liquid polyacrylamide phase into a spongelike pectin scaffold left residual filamentous networks of polyacrylamide imprinted in the pore spaces of the scaffold. This procedure limits the effect of freeze-drying on possible mechanical damage to the physical structure of the resulting composite.

Finally, we believe the methodology developed here could prevent the irreversible deactivation of poly-

mers during lyophilization. Deactivation may occur during formulation in carrier systems of many environmentally sensitive biomacromolecules including proteins, polypeptides, and others.

References

1. Vandamme; Th. F.; Lenourry, A.; Charrueau, C.; Chaumeil, J.-C. Carbohydr Polym 2002, 48, 219.
2. Christensen, S. H. In: Food Hydrocolloids III; Glicksman, M., Ed.; CRC Press: Boca Raton, FL, 1984; Chapter 9.
3. Singh, R. P.; Tripathy, T.; Karmakar, G. P.; Rath, S. K.; Karmakar, N. C.; Pandey, S. R.; Kannan, K.; Jain, S. K.; Lan, N. T. Curr Sci 2000, 78, 798.
4. Semdè, R.; Amighi, A.; Devleeschouwer, M. J.; Moës, A. J. Int J Pharm 2000, 197, 169.
5. Sinha, V. R.; Kumira, R. Int J Pharm 2001, 224, 19.
6. Dhara, D.; Rathna, G. V. N.; Chatterji, P. R. Langmuir 2000, 16, 2424.
7. Kost, J.; Langer, R. Adv Drug Deliv Rev 2001, 46, 125.
8. Chen, G.; Imanishi, Y.; Ito, Y. Macromolecules 1998, 31, 4379.
9. Pappas, N. A.; Langer, R. Science 1994, 264, 1715.
10. Jeong, B.; Bae, Y. H.; Lee, D. S.; Kim, S. W. Nature 1997, 388, 860.
11. Hu, Z.; Zhang, X.; Li, Y. Science 1995, 269, 525.
12. Zecca, M.; Biffs, A.; Palma, G.; Corvaja, C.; Lora, S.; Jerabek, K.; Corain, B. Macromolecules 1996, 29, 4655.
13. Cohen, Y.; Ramon, O.; Kopelman, I. J.; Mizrahi, S. J Polym Sci Part B: Polym Phys 1992, 30, 1055.
14. Johansson, G. In: Partitioning in Aqueous Two-Phase Systems; Walter, H.; Brooks, D. E.; Fisher, D., Eds.; Academic Press: New York, 1985; Chapter 7.
15. Malik, M. A.; Nadler, A.; Letey, J. Soil Technol 1991, 4, 255.
16. Kajiwara, K.; Ross-Murphy, S. B. Nature 1992, 355, 208.
17. Chan, G. Y. N.; Kambouris, P. A.; Looney, M. G.; Qiao, G. G.; Solomon, D. H. Polymer 2000, 41, 27.
18. Elisseeff, J.; McIntosh, W.; Anseth, K.; Riley, S.; Ragan, P.; Langer, R. J Biomed Mater Res 2000, 51, 164.
19. Miyata, T.; Uragami, T.; Nakamae, K. Adv Drug Deliv Rev 2002, 54, 79.
20. Lapsley, K. G.; Escher, F. E.; Hoehn, E. Food Struct 1992, 11, 339.
21. Marle, J. T. V.; Clerkx, A. C. M.; Boekestein, A. Food Struct 1992, 11, 209.
22. Brandrup, J.; Immergut, E. H. Eds. Polymer Handbook; Wiley: New York, 1975; pp. III–146.
23. Diez-Pena, F.; Quijada-Garrido, I.; Frutos, P.; Barrales-Rienda, J. M. Macromolecules 2002, 35, 2667.
24. Garces, F. O.; Sivadasan, K.; Somasundaran, P.; Turro, N. J. Macromolecules 1994, 27, 272.
25. Garay, M. T.; Llamas, M. C.; Iglesias, E. Polymer 1997, 38, 5091.
26. Rinaudo, M. In: Pectin and Pectinases; Visser, J.; Voragen, A. G. J., Eds.; Elsevier Science: New York, 1996; Chapter 2.
27. Fishman, M. L.; Cooke, P.; Levaj, B.; Gillespie, D. T.; Sondey, S. M. Arch Biochem Biophys 1992, 294, 253.
28. Fishman, M. L.; Cooke, P.; Hotchkiss, A.; Damert, W. Carbohydr Res 1993, 248, 303.
29. Fishman, M. L.; Chau, H. K.; Hoagland, P.; Ayyad, K. Carbohydr Res 2000, 323, 126.
30. Fishman, M. L.; Chau, H. K.; Kolpak, F.; Brady, J. J Agric Food Chem 2001, 49, 4494.
31. Yalpani, M. Polysaccharides; Elsevier: New York, 1988; Chapter 4.
32. Mallam, A.; Horkay, F.; Hecht, A.-M.; Geissler, E. Macromolecules 1989, 22, 3356.
33. BeMiller, J. M. In: Chemistry and Function of Pectins; Fishman, M. L., Ed.; American Chemical Society: Washington, DC, 1986; Chapter 1.
34. Round, A. N.; MacDougall, A. J.; Ring, S. G.; Morris, V. J. Carbohydr Res 1997, 303, 251.
35. Walkinshaw, M. D.; Arnott, S. J Mol Biol 1981, 153, 1055.
36. Walkinshaw, M. D.; Arnott, S. J Mol Biol 1981, 153, 1075.
37. Fishman, M. L.; Coffin, D. R.; Unruh, J. J.; Ly, T. J Macromol Sci Pure Appl Chem 1996, A33, 639.